THE JOURNAL OF BIOLOGICAL CHEMISTRY VOL. 287, NO. 35, pp. 29702–29712, August 24, 2012
© 2012 by The American Society for Biochemistry and Molecular Biology, Inc. Published in the U.S.A.

Dopamine Transporter Phosphorylation Site Threonine 53 Regulates Substrate Reuptake and Amphetamine-stimulated Efflux*

Received for publication, March 29, 2012, and in revised form, June 13, 2012 Published, JBC Papers in Press, June 21, 2012, DOI 10.1074/jbc.M112.367706

James D. Foster[‡1], Jae-Won Yang[§1], Amy E. Moritz[‡], Sathyavathi ChallaSivaKanaka[‡], Margaret A. Smith[‡], Marion Holy[§], Kyle Wilebski[‡], Harald H. Sitte[§2,3], and Roxanne A. Vaughan[‡2,4]

From the [‡]Department of Biochemistry and Molecular Biology, University of North Dakota School of Medicine and Health Sciences, Grand Forks, North Dakota 58202-9037 and the [§]Center of Physiology and Pharmacology, Institute of Pharmacology, Medical University Vienna, Waehringerstrasse 13a, A-1090 Vienna, Austria

Background: DAT activity is regulated by protein kinases.
Results: We identify Thr^{53} as a DAT phosphorylation site in rat striatum by mass spectrometry and a phospho-specific antibody; Thr^{53} mutation reduced dopamine influx and ablated transporter-mediated efflux.
Conclusion: Phosphorylation of DAT Thr^{53} is involved in transport activity.
Significance: These results identify Thr^{53} phosphorylation of DAT *in vivo* and elucidate associated functional properties.

In the central nervous system, levels of extraneuronal dopamine are controlled primarily by the action of the dopamine transporter (DAT). Multiple signaling pathways regulate transport activity, substrate efflux, and other DAT functions through currently unknown mechanisms. DAT is phosphorylated by protein kinase C within a serine cluster at the distal end of the cytoplasmic N terminus, whereas recent work in model cells revealed proline-directed phosphorylation of rat DAT at membrane-proximal residue Thr^{53}. In this report, we use mass spectrometry and a newly developed phospho-specific antibody to positively identify DAT phosphorylation at Thr^{53} in rodent striatal tissue and heterologous expression systems. Basal phosphorylation of Thr^{53} occurred with a stoichiometry of ~50% and was strongly increased by phorbol esters and protein phosphatase inhibitors, demonstrating modulation of the site by signaling pathways that impact DAT activity. Mutations of Thr^{53} to prevent phosphorylation led to reduced dopamine transport V_{max} and total apparent loss of amphetamine-stimulated substrate efflux, supporting a major role for this residue in the transport kinetic mechanism.

The neurotransmitter dopamine (DA)[5] plays a key role in many brain processes, including motor activity, motivation, and reward. Proper dopaminergic function is dependent on the reuptake activity of the dopamine transporter (DAT), which is the primary mechanism responsible for spatial and temporal control of extraneuronal DA (1–3). Dysregulation of transport activity and consequent DA imbalance are hypothesized to contribute to dopaminergic disorders, such as Parkinson disease, depression, attention deficit hyperactivity disorder, and schizophrenia (4–6). DAT is also a target for many drugs of abuse, such as cocaine and amphetamine (AMPH), and for therapeutic agents used to treat DA diseases (7, 8). In particular, AMPH and its congeners induce multiple acute and chronic effects on DAT (9), including reversal of transport direction (10), that lead to substrate efflux and depletion of transmitter stores (11). The mechanism underlying efflux remains to be elucidated, but it is associated with transporter-generated currents (12) that correlate with substrate-releasing capacity (13) and involves N-terminal serine phosphorylation (14).

DAT is subject to extensive acute and chronic regulation that modulates DA neurotransmission in response to momentary physiological demands and to long term disease or drug addiction states (7, 15, 16). Changes in DAT activity and cell surface expression occur in response to the actions of several kinases and phosphatases, including protein kinase C (PKC), extracellular signal-related kinase (ERK), and protein phosphatases 1 and 2A (PP1/2A) (17–20). DAT is phosphorylated in PKC- and phosphatase-dependent manners, but the mechanistic relationships between transporter phosphorylation and regulation remain unclear. Using $^{32}PO_4$ metabolic labeling, we have found in rat striatal tissue and model cells that ~90% of rDAT phosphorylation occurs on phosphoserine (Ser(P)) and ~10% occurs on phosphothreoine (Thr(P)) (17, 21). Phosphorylation occurs at a tonic level that is increased with PKC activators, PP1 inhibitors, and *in vitro* and *in vivo* administration of AMPH (22), with the majority of ^{32}P labeling occurring in a serine cluster at the distal end of the N-terminal domain (21–23). We

* This work was supported, in whole or in part, by National Institutes of Health, Grant R01 DA13147 from NIDA (to R. A. V.), ND EPSCoR IIG (to R. A. V. and J. D. F.), P20 RR017699 from the COBRE program of the National Center for Research Resources (to the University of North Dakota), and P20 RR016741 from the IDeA Networks of Biomedical Research Excellence (INBRE) program of the National Center for Research Resources (to the University of North Dakota). This work was also supported by Austrian Research Funds/FWF Grants F3506 and P22893-B1 (to H. H. S.) and P23670-B09 (to J.-W. Y.).
⌘ *Author's Choice*—Final version full access.
[1] Both authors contributed equally to this work.
[2] Both authors contributed equally to this work.
[3] To whom correspondence may be addressed. Tel.: 43-1-4277-64123; Fax: 43-1-4277-9641; E-mail: harald.sitte@meduniwien.ac.at.
[4] To whom correspondence may be addressed. Tel.: 701-777-3419; Fax: 701-777-2382; E-mail: roxanne.vaughan@med.und.edu.
[5] The abbreviations are: DA, dopamine; DAT, dopamine transporter; PMA, phorbol 12-myristate 13-acetate; OA, okadaic acid; AMPH, amphetamine; MPP^+, [^{3}H]1-methyl-4-phenylpyridinium; NDAT, recombinant DAT N-terminal tail protein; rDAT, rat DAT; SH3, Src homology 3; TM1, transmembrane domain 1; Ab, antibody; ANOVA, analysis of variance.

recently showed that a recombinant peptide containing N-terminal residues 1–65 of rDAT (NDAT) was phosphorylated *in vitro* by the proline-directed kinases ERK1/2, JNK, and p38 MAPK, which require a proline immediately C-terminal to the phosphate acceptor (24–28). We identified the membrane-proximal residue Thr^{53}, which precedes Pro^{54}, as the NDAT ERK phosphorylation site (29) and showed the apparent total loss of Thr(P) from $^{32}PO_4$ metabolically labeled rDAT carrying a Thr^{53} → Ala mutation, indicating that Thr^{53} is a major site or the sole site of Thr(P) in the heterologously expressed protein (29).

In this study, we use mass spectrometry and a phosphospecific antibody as positive function approaches to demonstrate Thr^{53} phosphorylation of DAT and examine its characteristics without the necessity for $^{32}PO_4$ labeling or interference from PKC-induced Ser phosphorylation. Our findings verify *in vivo* phosphorylation of DAT Thr^{53} in rat and mouse striatum as well as in heterologous model cells and demonstrate its modulation by signaling pathways. DAT mutants containing non-phosphorylatable residues at position 53 possessed reduced DA transport V_{max} and in superfusion assays showed complete loss of AMPH-induced substrate efflux, suggesting a crucial role for this residue in transport kinetics. These findings reveal Thr^{53} phosphorylation as a novel mechanism for regulation of DAT functions and identify the membrane-proximal region of the N terminus as a major locus for regulation of transport kinetics.

EXPERIMENTAL PROCEDURES

Animals and Materials—Protein G- and protein A-Sepharose beads were from GE Healthcare; PMA, OA, recombinant PKCα, and ERK1 were from EMD Calbiochem; goat anti-DAT polyclonal antibody (C-20) was from Santa Cruz Biotechnology, Inc. (Santa Cruz, CA); Colorburst molecular mass standards, alkaline phosphatase-linked anti-mouse and anti-rabbit IgG antibodies, and other fine chemicals were from Sigma-Aldrich; FuGENE 6 transfection reagent and Complete Mini protease inhibitor tablets were from Roche Applied Science; bicinchoninic acid (BCA) protein assay reagent was from Thermo Scientific; [7,8-^{3}H]DA (45 Ci/mmol) was from GE Healthcare; and [^{125}I]RTI82 was synthesized and radioiodinated as previously described (30). The recombinant NDAT was prepared and subjected to *in vitro* phosphorylation with PKC and ERK1 as described previously (29). Rats were purchased from Charles River Laboratories or the Institute for Animal Genetics, Medical University of Vienna (Himberg), and SV129 mice were obtained from Dr. Eric Murphy (University of North Dakota). All animals were housed and treated in accordance with regulations established by the National Institutes of Health and approved by the University of North Dakota Institutional Animal Care and Use Committee.

Cell Culture and DAT Mutagenesis—Lewis lung carcinoma-porcine kidney (LLC-PK$_1$) cells or LLC-PK$_1$ cells stably expressing WT rDAT (rDAT-LLCPK$_1$) (31) or T53A or T53D rDAT were maintained in α-minimum essential medium supplemented with 5% fetal bovine serum, 2 mM L-glutamine, 200 μg/ml G418, and 100 μg/ml penicillin/streptomycin. tsA201 cells were cultured in Dulbecco's modified Eagle's medium (DMEM) with 10% FBS and penicillin/streptomycin. Cells were maintained in a humidified incubation chamber gassed with 5% CO_2 at 37 °C. The T53A, T53D, and T53E mutations were made in the rDAT pcDNA 3.0 template using the Stratagene QuikChange® kit with codon substitution verified by sequencing (Alpha Biolabs, Northwoods DNA). For production of pooled stable transformants, transfected cells (FuGENE, Roche Applied Science) were maintained under selection with 800 μg/ml G418 (29). tsA201 cells were transiently transfected with WT rDAT using the ExGen500 reagent (Fermentas) according to the manufacturer's protocol. For experiments with T53E, LLC-PK$_1$ cells were transiently transfected with 0.6 μg of WT or T53E DNA/well using FuGENE and assayed for [^{3}H]DA transport activity after 24 h.

Tandem Mass Spectrometry Analysis (LC-MS/MS)—Rat striatal synaptosomes, rDAT-LLCPK$_1$ cells, or tsA201 cells transiently expressing rDAT were solubilized in lysis buffer containing 1% Triton X-100, 20 mM Tris-HCl (pH 8.0), 150 mM NaCl, 1 mM EDTA, 1 mM sodium orthovanadate, 5 mM sodium fluoride, 5 mM sodium pyrophosphate, and a protease inhibitor mixture (Roche Applied Science) on a tube rotator for 2 h at 4 °C. After centrifugation at 14,000 × *g* for 30 min at 4 °C, the supernatant was collected and incubated overnight with a goat anti-DAT polyclonal antibody. Immune complexes were collected with protein G beads and washed extensively, and bound proteins were eluted in Laemmli buffer (63 mM Tris-HCl, 10% glycerol, 2% SDS, 3% 2-mercaptoethanol, 100 mM dithiothreitol, 0.0025% bromphenol blue, pH 6.8) at 95 °C for 3 min. Eluted proteins were size-fractionated on SDS-polyacrylamide gels and visualized by Coomassie Brilliant Blue staining, and the indicated band was excised. Gel pieces were destained with 50% acetonitrile in 25 mM ammonium bicarbonate and dried in a speed vacuum concentrator. After reduction and alkylation of cysteine residues, gel pieces were washed and dehydrated. Dried gel pieces were rehydrated with 25 mM ammonium bicarbonate (pH 8.0) containing 10 ng/μl trypsin or chymotrypsin (Promega, Madison, WI) and incubated for 18 h at 37 °C. The digested peptide mixtures were extracted with 50% acetonitrile in 5% formic acid and concentrated in a speed vacuum concentrator for LC-MS/MS. An ion trap mass spectrometer (HCT, BrukerDaltonics, Bremen, Germany) coupled with an Ultimate 3000 nano-HPLC system (Dionex, Sunnyvale, CA) was used for LC-MS/MS data acquisition. A PepMap100 C-18 trap column (300 μm × 5 mm) and PepMap100 C-18 analytic column (75 μm × 150 mm) were used for reverse phase chromatographic separation with a flow rate of 300 nl/min. The two buffers used for the reverse phase chromatography were 0.1% formic acid, water (buffer A) and 0.08% formic acid, acetonitrile (buffer B) with a 125 min gradient (4–30% B for 105 min, 80% B for 5 min, and 4% B for 15 min). Eluted peptides were then directly sprayed into the mass spectrometer to record peptide spectra over the mass range of m/z 350–1500 and MS/MS spectra in information-dependent data acquisition over the mass range of m/z 100–2800. Repeatedly, MS spectra were recorded, followed by three data-dependent collision-induced dissociation MS/MS spectra generated from the four highest intensity precursor ions. The MS/MS spectra were interpreted with the Mascot search engine (Matrix Science, London, UK). Data base searches through Mascot were performed with a mass toler-

ance of 0.5 Da and an MS/MS tolerance of 0.5 Da; three missing cleavage sites and carbamidomethylation on cysteine, oxidation on methionine, deamidation on asparagine/glutamine, and phosphorylation on serine/threonine were allowed. Each filtered MS/MS spectra exhibiting possible phosphorylation was manually checked and validated (32, 33).

Phospho-specific Antibody Generation—A Threonine 53-phosphospecific polyclonal antibody (Thr(P)^{53} Ab) against DAT was generated by PhosphoSolutions (Aurora, CO). Briefly, rabbits were immunized with a phosphopeptide based on the DAT N-terminal amino acid sequence: TNSTLINPPQ**pT**PVEAQERTW (Thr(P)^{53} shown in boldface type). Control peptide consisting of the identical sequence with non-phosphorylated Thr^{53} was also synthesized. Thr(P)^{53}-specific polyclonal antibody present in immune serum was purified through sequential rounds of chromatography against immobilized phospho- and dephosphopeptide and concentrated to 1 mg/ml. Affinity-purified antibody screened by ELISA showed strong reactivity against the Thr(P)^{53} peptide antigen and essentially no reactivity to the corresponding dephosphopeptide (not shown).

DAT Immunoblot and Immunoprecipitation—Immunoblotting was performed with mouse monoclonal N-terminal Ab 16 (mAb 16) generated against residues 42–59 to detect total DAT as described previously (34) or with rabbit polyclonal Thr(P)^{53} Ab generated in this study. Briefly, lysates of rodent striatal membranes or rDAT-LLCPK$_1$ cells were resolved on 4–20% SDS-polyacrylamide gels using ColorBurst (Sigma) molecular mass markers as standards. For regulation studies, rat striatal synaptosomes were prepared and treated with vehicle, phorbol 12-myristate 13-acetate (PMA), or okadaic acid (OA) for 30 min at 30 °C as described previously (35), followed by lysis and electrophoresis. Gels were transferred to PVDF and blocked, followed by incubation with primary antibodies used at 1:1000 dilutions. Where indicated, N-terminal peptides with or without Thr^{53} phosphorylation were included with the primary antibodies at 50 μg/ml. Immunostaining was detected using anti-mouse or anti-rabbit alkaline phosphatase-conjugated secondary antibodies and chemiluminescent light detection using ImmunStar (Bio-Rad) substrate and a Bio-Rad gel documentation system. For quantification of Thr^{53} phosphorylation, Thr(P)^{53} Ab staining was normalized to total DAT levels determined in parallel using mAb 16, and statistical analysis was performed using ANOVA. For immunoprecipitation studies, lysates of unlabeled or [^{125}I]RTI82-labeled rat striatal membranes (36) were immunoprecipitated with polyclonal Ab 16 or Thr(P)^{53} Ab (3 μg) using procedures previously described (37). Precipitated DATs were resolved on 4–20% SDS-polyacrylamide gels and were transferred for subsequent immunoblotting or were dried and exposed to x-ray film for 3–7 days at −80 °C.

Determination of Thr^{53} Phosphorylation Stoichiometry—Rat striatal lysates were immunoprecipitated with Thr(P)^{53} Ab, and bound and unbound fractions were immunoblotted with Thr(P)^{53} Ab to determine the fraction of Thr^{53}-phosphorylated transporters retained in the pellet. Bound samples were also blotted with mAb 16 to detect total DAT protein in the pellet, and the fraction of input DAT pulled down by Thr(P)^{53} Ab was determined by comparing the staining intensities of the Thr(P)^{53} Ab pellet with that of a DAT standard curve generated by titration of input sample and immunoblotted in parallel with mAb 16. The Thr(P)^{53} stoichiometry estimate was determined by dividing the fraction of input DAT present in the Thr(P)^{53} Ab pellets by the Thr(P)^{53} Ab precipitation efficiency.

DA Uptake and Cell Surface Biotinylation Assays—WT or mutant rDAT-LLCPK$_1$ cells were grown in 24-well plates to 70–80% confluence in α-minimum essential medium at 37 °C. Cells were rinsed twice with 0.5 ml of Krebs-Ringer-HEPES (KRH) buffer (25 mM HEPES, 125 mM NaCl, 4.8 mM KCl, 1.2 mM KH_2PO_4, 1.3 mM $CaCl_2$, 1.2 mM $MgSO_4$, 5.6 mM glucose, pH 7.4) followed by the addition of 0.5 ml of warmed KRH buffer (37 °C) and uptake assay. Uptake was performed in triplicate and initiated by the addition of 10 nM [^{3}H]DA plus 0.3–30 μM unlabeled DA (where indicated). Nonspecific uptake was determined in the presence of 100 μM (−)-cocaine. Uptake was allowed to proceed for 8 min at 37 °C, and cells were rapidly washed three times with ice-cold KRH buffer. Cells were solubilized in 1% Triton X-100, radioactivity contained in lysates was assessed by liquid scintillation counting, and protein content was assessed using BCA colorimetric reagent. For cell surface expression determination, WT or mutant rDAT-LLCPK$_1$ cells were incubated with the membrane-impermeable biotinylating reagent sulfosuccinimidyl-2[biotinamido]ethyl-1,3-dithiopropionate sulfo-NHS-SS-biotin, and biotinylated DATs were purified from cell lysates (25 μg of protein) by chromatography on NeutrAvidin beads, separated by SDS-PAGE, and quantified by immunoblotting (38). For ion dose-response experiments, Na^+ and Cl^- were replaced across the range of 0–150 mM with *N*-methyl D-gluconate or sodium acetate, respectively, and uptake was analyzed using 10 nM [^{3}H]DA plus 3 μM DA (39, 40).

Superfusion Experiments—Substrate efflux assays were performed as previously described (41). In brief, culture medium was removed from stably transfected WT or mutant rDAT LLC-PK$_1$ cells (see above; 4×10^5 cells/well grown on coverslips in 96-well plates) and exchanged with KRH buffer. In all superfusion assays, we used [^{3}H]1-methyl-4-phenylpyridinium (MPP^+) (85 Ci/mmol; American Radiolabeled Chemicals, St. Louis, MO) as the DAT substrate because it is metabolically inert, cannot diffuse out of the cells, and thereby significantly enhances the signal/noise ratio of the experiment (42). The cells were preincubated with 0.1 μM MPP^+ for 20 min at 37 °C in a final volume of 0.1 ml of KRH buffer/well and subsequently transferred into superfusion chambers. Immediately, superfusion was initiated with KRH buffer at 25 °C at a perfusion rate of 0.7 ml/min. After 45 min, a stable efflux of radioactivity was achieved, and the experiment was started with the collection of 2-min fractions. After three fractions, AMPH (3 μM) was added to stimulate the reverse operation of DAT.

RESULTS

Identification of Phosphorylated Thr^{53} on DAT by Mass Spectrometry—To identify *in vivo* DAT phosphorylation, we immunopurified DAT from rat striatal lysates and size-fractionated purified proteins by SDS-PAGE (Fig. 1*A*). The indicated Coomassie Blue-stained band was subjected to trypsin in-gel digestion, and resulting peptides were subjected to liquid

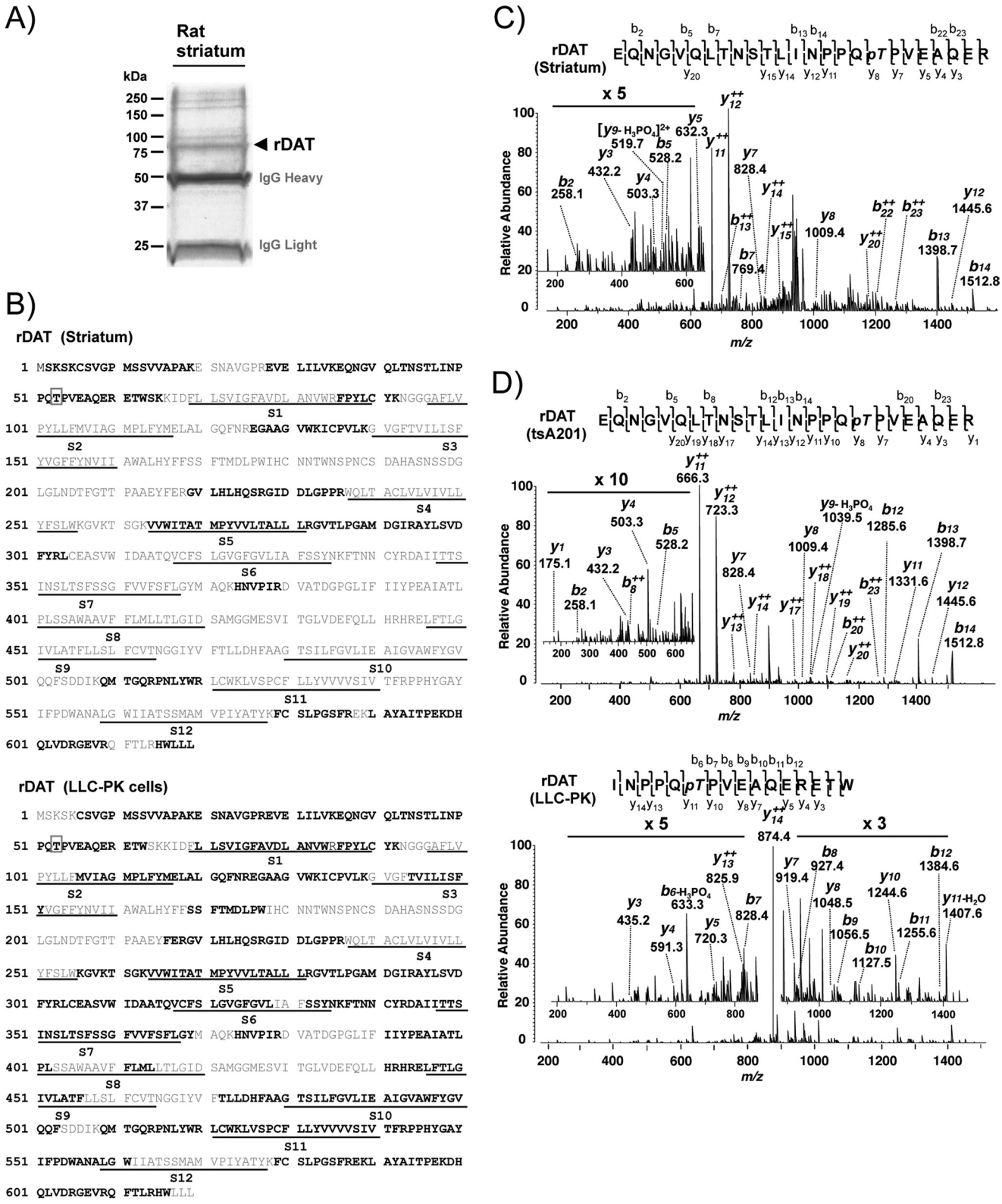

FIGURE 1. **Identification of Thr[53] phosphorylation of DAT in rat striatum and heterologous cells by LC-MS/MS.** *A*, Coomassie Blue-stained SDS-PAGE gel with immunopurified rat striatal DAT (*arrow*). Molecular mass markers are indicated on the *left*. *B*, sequence coverage of DAT with identified peptides (*boldface type*) by MS/MS from rat striatum (*top*) and rDAT-LLCPK$_1$ cells (*bottom*). The putative 12 transmembrane segments (*S1–S12*) of DAT are *underlined*, and the identified phosphorylation site at Thr^{53} is indicated by a *box*. *C*, the spectrum of triple charged rDAT peptide obtained at *m/z* 948.45 was fragmented to produce a tandem mass spectrum with *y*- and *b*-ion series. The MS/MS spectrum shows phosphorylated Threonine (pT) in the sequence EQNGVQLTNSTLINPPQpTPVEAQER (amino acids 36–60). *D*, MS/MS spectrum from rDAT transiently expressed in tsA201 cells (*top*) and stably expressed in LLC-PK$_1$ cells (*bottom*). The triple charged, tryptic peptide at *m/z* 948.44 from heterologous tsA201 cells was fragmented to *y*- and *b*-ion series that described the sequence EQNGVQLTNSTLINPPQpTPVEAQER with phosphorylation at Thr^{53}. In rDAT-LLCPK$_1$ cells, the spectrum of double charged, chymotryptic peptide at *m/z* 987.99 presents the unambiguous identification of Thr(P)^{53} in the sequence INPPQpTPVEAQERETW of rDAT.

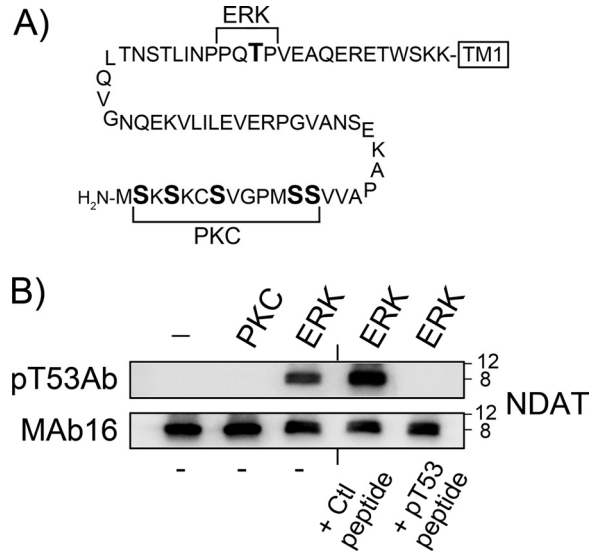

FIGURE 2. **Immunoreactivity of NDAT with Thr(P)^{53} Ab.** *A*, rat DAT N-terminal amino acid sequence (residues 1–65; *NDAT*) highlighting the PKC-dependent phosphorylation domain (*PKC*) and the ERK proline-dependent phosphorylation site (*ERK*). *B*, NDAT samples given no kinase treatments or phosphorylated *in vitro* by PKCα or ERK1 were immunoblotted with Thr(P)^{53} Ab (*pT53Ab*) (*top*) or mAb 16 (*bottom*). Where indicated, Thr(P)^{53} Ab was preincubated with phosphorylated (*pT53*) or non-phosphorylated (*Ctl*) N-terminal peptide. Molecular mass markers are indicated on the *right*.

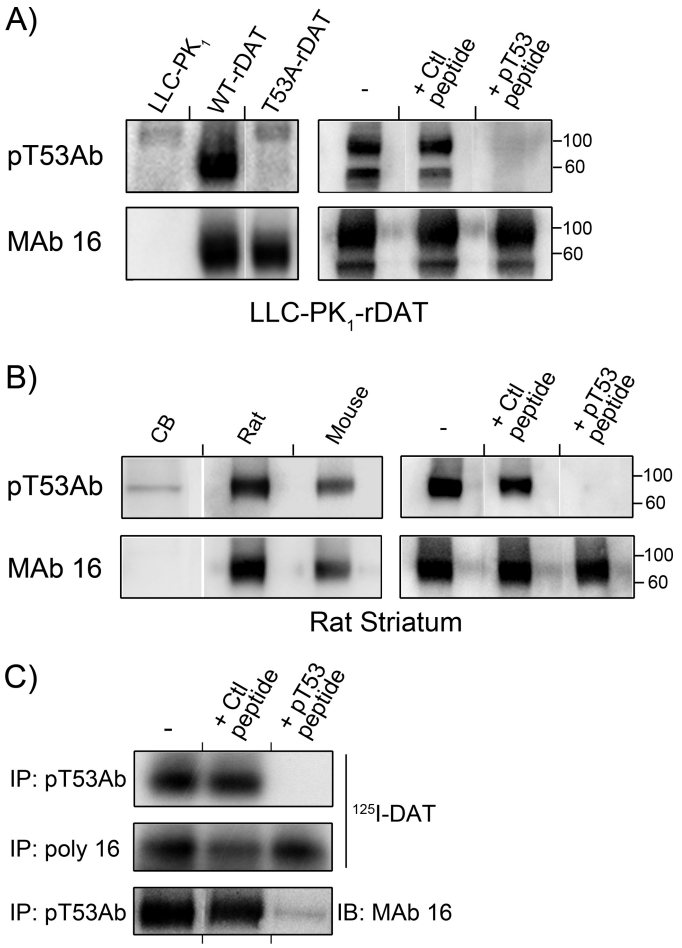

FIGURE 3. **Immunoreactivity of DAT with Thr(P)^{53} Ab.** Lysates from LLC-PK$_1$ cells, rDAT-LLCPK$_1$ cells, or T53A rDAT-LLCPK$_1$ cells (*A*) or lysates from rDAT-LLCPK$_1$ cells (*B*) were immunoblotted with Tyr(P)^{53} Ab (*pT53Ab*) (*top panels*) or mAb 16 (*bottom panels*). Where indicated, Thr(P)^{53} Ab was preincubated with phosphorylated (*pT53*) or non-phosphorylated (*Ctl*) N-terminal peptide. Molecular mass markers are indicated on the *right*. *C* and *D*, lysates from rat or mouse striatal or rat cerebellar (*CB*) tissue were immunoblotted with Thr(P)^{53} Ab (*top panels*) or mAb 16 (*bottom panels*). Where indicated, Thr(P)^{53} Ab was preincubated with phosphorylated (*pT53*) or non-phosphorylated (*Ctl*) N-terminal peptide. Molecular mass markers are indicated on the *right*. *E*, rat striatal membranes with (*top* and *middle panels*) or without (*bottom panel*) [^{125}I]RTI-82 photoaffinity labeling of DAT were immunoprecipitated (*IP*) with Thr(P)^{53} Ab or polyclonal Ab 16 as indicated and resolved by SDS-PAGE. Gels were dried and subjected to autoradiography (*top* and *middle panels*) or transferred to PVDF and probed with mAb 16 (*bottom panels*). Where indicated, Thr(P)^{53} Ab was preincubated with phosphorylated (*pT53*) or non-phosphorylated (*Ctl*) N-terminal peptide.

chromatography tandem MS (LC-MS/MS). LC-MS/MS identified DAT protein (Swiss-Prot ID: P23977) with 97 matched peptides and 30.2% sequence coverage (Fig. 1*B*, *top*). Thr(P) was unambiguously and repeatedly identified at residue 53 in the MS/MS spectra of the tryptic peptide spanning amino acid residues 30–60 (EQNGVQLTNSTLINPPQ**pT**PVEAQER) (Fig. 1*C*). To confirm phosphorylation of DAT at Thr^{53} in heterologous cells, we also analyzed rDAT transiently or stably expressed in mammalian cell lines. Using the same MS approach, we found that DAT was phosphorylated at Thr^{53} in both tsA201 and rDAT-LLCPK$_1$ cell lines (Fig. 1*D*). The use of chymotrypsin for in-gel digestion substantially increased sequence coverage. MS/MS analysis mapped rDAT protein with individual sequence coverage of 30.7 and 52.7% for tryptic and chymotryptic peptides, respectively (data not shown), summing up to a total sequence coverage of 68.7% of the rDAT protein in rDAT-LLCPK$_1$ cells with Thr(P)^{53} (Fig. 1*B*, *bottom*).

Characterization of Thr(P)^{53} Ab Immunoreactivity—We then assessed the ability of our phospho-specific antibody to detect Thr(P)^{53} in the DAT sequence. In our previous study (29), we demonstrated that the recombinant N-terminal domain peptide NDAT was phosphorylated *in vitro* by ERK1/2 at Thr^{53}, whereas more recently we have determined that PKC-catalyzed phosphorylation of NDAT occurs on multiple sites in the distal serine cluster, paralleling PKC-induced metabolic phosphorylation of this domain (21) (Fig. 2*A*). We used these differentially phosphorylated NDAT samples to test the specificity of the Thr(P)^{53} Ab in immunoblot assays. Thr(P)^{53} Ab did not recognize NDAT that was not phosphorylated or was phosphorylated by PKC, but it was strongly reactive against ERK-phosphorylated NDAT (Fig. 2*B*, *top*). Staining of ERK-phosphorylated NDAT was lost when Thr(P)^{53} Ab was preincubated with Thr(P)^{53} peptide but was not affected by incubation with the corresponding dephosphopeptide (Fig. 2*B*, *top*). Staining of blots with mAb 16 verifies equal NDAT protein in all samples (Fig. 2*B*, *bottom*) and demonstrates the upward shift of NDAT induced by Thr^{53} phosphorylation that we previously reported (29). These results demonstrate that Thr(P)^{53} Ab specifically recognizes DAT N-terminal tail sequence phosphorylated at Thr^{53} and does not recognize N-terminal sequence that is not phosphorylated or is phosphorylated by PKC on distal serines.

Thr(P)^{53} Ab Staining of Expressed DAT—We then assessed the ability of Thr(P)^{53} Ab to recognize DAT expressed heterologously in LLCPK$_1$ cells (Fig. 3*A*). Thr(P)^{53} Ab produced little or no immunostaining of lysates from LLCPK$_1$ cells but showed strong immunoreactivity against a ~90 kDa band in rDAT-LLCPK$_1$ lysates, indicating specific recognition of rDAT (Fig.

3*A*, *upper panels*). Importantly, Thr(P)[53] Ab showed no reactivity against T53A rDAT (Fig. 3*A*, *left*), and immunostaining of WT DAT was prevented by inclusion of Thr(P)[53] peptide but not by the corresponding dephosphopeptide (Fig. 3*A*, *right*). Equal levels of WT and T53A rDAT protein and the absence of rDAT in $LLCPK_1$ cells are shown by mAb 16 staining (Fig. 3*A*, *bottom panels*). These results demonstrate high specificity of the Thr(P)[53] Ab toward phosphorylated Thr[53] of rDAT, confirming the mass spectrometry results and supporting our previous loss-of-function evidence for Thr[53] phosphorylation in expressed DAT (29).

We also noted in these experiments that Thr(P)[53] Ab stained the unglycosylated 60-kDa form of DAT as well as the fully glycosylated 90-kDa form (Fig. 3*A*, *right*). The ratio of mature and immature form staining by Thr(P)[53] Ab was comparable with that detected by mAb 16, indicating that both forms possess similar levels of Thr[53] phosphorylation. We also frequently observed a minor band at >100 kDa in parent cell and T53A rDAT lysates (Fig. 3*A*, *left*), indicating the presence of a small degree of cross-reactivity of this Ab with another protein. However the intensity of this staining is negligible in comparison with that of DAT.

Thr(P)[53] Ab Staining of Rat and Mouse Striatal DAT—Next we immunoblotted rat and mouse striatal DAT with Thr(P)[53] Ab (Fig. 3*B*). Thr(P)[53] Ab was highly reactive against a protein of ~90 kDa from rat striatal tissue, with only negligible staining detected in cerebellar tissue, which does not express DAT (Fig. 3*B*, *left*), strongly supporting the identity of the band as DAT. Staining of the rat striatal band was blocked by inclusion of Thr(P)[53] peptide but not by the dephosphopeptide (Fig. 3*B*, *right*), demonstrating Ab specificity for phosphorylated Thr[53]. Levels of DAT protein in each lane are indicated by mAb 16 staining (*bottom panels*). Mouse DAT, which possesses the Thr[53]-Pro[54] sequence (43), also showed strong immunoreactivity with Thr(P)[53] Ab (Fig. 3*B*, *left*), whereas human DAT, which possesses the sequence Ser[53]-Pro[54] (44), did not show Thr(P)[53] Ab immunostaining (not shown), further supporting the Ab specificity for Thr(P)[53]. Staining of a minor band in the cerebellar sample in the absence of DAT (Fig. 3*B*, *right*) further indicates a slight reactivity of this Ab with a different protein.

Immunoprecipitation of Rat Striatal DAT with Thr(P)[53] Ab—We also demonstrated the ability of Thr(P)[53] Ab to immunoprecipitate DAT (Fig. 3*C*). Thr(P)[53] Ab readily precipitated rat striatal DATs photoaffinity-labeled with the cocaine analog [^{125}I]RTI-82 (Fig. 3*C*, *top*) to levels that were comparable with that precipitated using our standard procedures with polyclonal Ab 16 (Fig. 3*C*, *middle*). Non-photolabeled rDATs precipitated by Thr(P)[53] Ab could also be detected by immunoblotting with mAb 16 (Fig. 3*C*, *bottom*). In both cases, Thr(P)[53] Ab-mediated precipitation was blocked with Thr(P)[53] peptide but not with the dephosphopeptide (Fig. 3*C*, *top*), demonstrating specificity for Thr[53] phosphorylation.

Modulation of Thr[53] DAT Phosphorylation—DAT phosphorylation has been studied primarily by metabolic labeling with $^{32}PO_4$ and has been demonstrated to be modulated by PKC, AMPH, and protein phosphatases (17, 21, 22, 45–47). However, the vast majority of basal and stimulated $^{32}PO_4$ labeling occurs on distal N-terminal serines (21), making this method unfeasible for characterization of Thr[53] phosphorylation responses. To examine the potential for Thr(P)[53] Ab to detect regulation of Thr[53] phosphorylation, rDAT-$LLCPK_1$ cells and rat striatal tissue were treated with OA to inhibit protein phosphatases or with PMA to activate PKC, followed by blotting with Thr(P)[53] Ab or mAb 16. OA and PMA treatments caused Thr[53] phosphorylation to increase to 178 ± 20% and 140 ± 13% of basal levels ($p < 0.01$ and $p < 0.05$, respectively) in rDAT-$LLCPK_1$ cells (Fig. 4*A*) and to 174 ± 15% and 168 ± 23% of basal levels ($p < 0.001$ and $p < 0.05$, respectively) in rat striatal synaptosomes (Fig. 4*B*). These results show the ability of Thr(P)[53] Ab to detect changes in Thr[53] phosphorylation levels and demonstrate the acute modulation of rDAT Thr[53] phosphorylation by PKC and phosphatase pathways in both expression systems and native tissue.

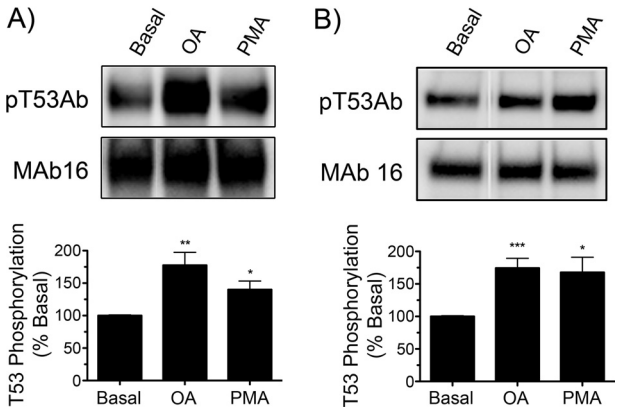

FIGURE 4. **Regulation of Thr[53] phosphorylation by phorbol ester and okadaic acid.** *A*, rDAT-$LLCPK_1$ cells were treated with vehicle, 1 μM OA, or 1 μM PMA for 30 min at 37 °C. *B*, rat striatal synaptosomes were treated with vehicle, 1 μM OA, or 1 μM PMA for 30 min at 30 °C. Lysates were subjected to SDS-PAGE and immunoblotted with Thr(P)[53] Ab (*pT53Ab*) (*top*) or mAb 16 (*bottom*) (representative examples shown). Histograms show quantification of Thr(P)[53] staining relative to vehicle controls (means ± S.E.; $n = 3$) (*, $p < 0.05$; **, $p < 0.01$; ***, $p < 0.001$ relative to basal by ANOVA).

Phosphorylation Stoichiometry—To obtain an estimate of basal phosphorylation stoichiometry, we analyzed lysates of untreated rat striatal tissue. Thr(P)[53] Ab was used to specifically extract Thr[53]-phosphorylated protein in immunoprecipitation procedures. Analysis of the bound and unbound fractions by Thr(P)[53] Ab immunoblotting showed that Thr[53]-phosphorylated DATs were captured with an efficiency of 38 ± 1%. The amount of total DAT in the precipitated sample was estimated to be 20 ± 1% of the input value, as determined by comparison of mAb 16 staining of Thr(P)[53] Ab pellets with DAT standard curves generated by dilutions of input striatal lysate and immunoblotted in parallel with mAb 16. Normalizing the fraction of DAT protein in the Thr(P)[53] Ab pellet by the Thr(P)[53] Ab precipitation efficiency yielded a Thr[53] phosphorylation stoichiometry estimate of 53 ± 2% (data not shown; all values means ± S.E. from three independent experiments performed in duplicate).

Kinetic Analysis of Thr[53] Mutants—To examine possible functions of Thr[53] phosphorylation, we generated T53A non-phosphorylatable and T53D phosphomimetic mutants for stable expression in $LLCPK_1$ cells. mAb 16 immunoblotting showed that T53A and T53D mutants co-migrated with the WT protein at ~90 kDa on SDS-polyacrylamide gels, indicating

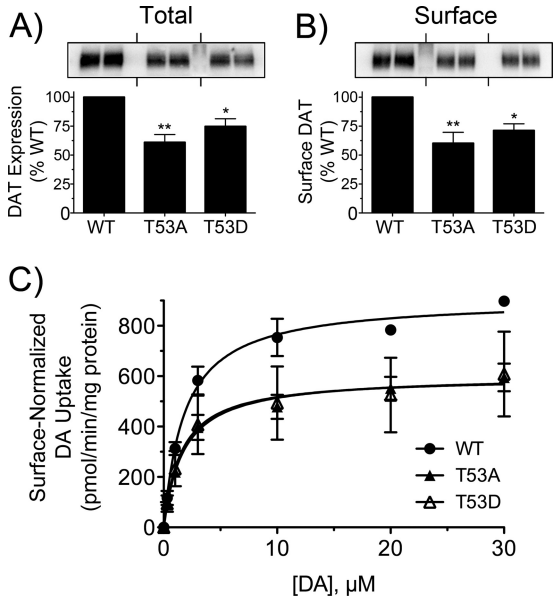

FIGURE 5. **Expression and kinetic analysis of T53A and T53D DATs.** rDAT-LLCPK$_1$ cells stably expressing WT, T53A, or T53D DATs were assayed in parallel for total DAT expression levels (*A*), surface DAT expression levels (*B*), and DA uptake saturation analysis (*C*). Blots shown are representative of four independent experiments with samples run in duplicate. Histograms show quantification of DAT levels (**, $p < 0.01$; *, $p < 0.05$ relative to controls by ANOVA with Tukey's post hoc test). Transport kinetic parameters were determined by nonlinear regression analysis in three or four independent experiments performed in triplicate. Data are presented as means ± S.E. normalized to cell surface DAT expression levels (**, $p < 0.01$; *, $p < 0.05$ relative to controls by ANOVA with Tukey's post hoc test).

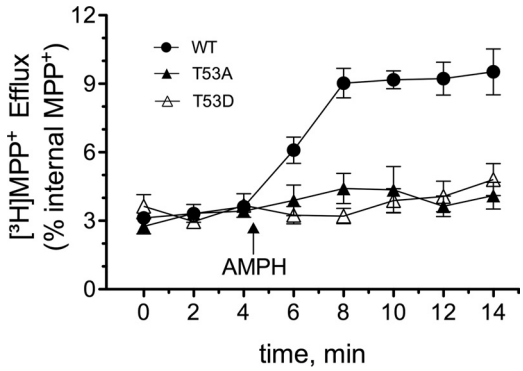

FIGURE 6. **Amphetamine-stimulated efflux of T53A and T53D DATs.** LLC-PK$_1$ cells stably expressing WT, T53A, or T53D DATs were preloaded with [^{3}H]MPP$^+$ for 20 min at 37 °C followed by superfusion analysis of efflux as described under "Experimental Procedures." Upon reaching a stable base line, three 2-min fractions were collected to define basal efflux followed by the addition of 3 μM AMPH (*arrow*) to stimulate DAT-mediated efflux.

full glycosylation and proper biosynthetic processing (48). Total expression levels of the mutants were 61 ± 7% and 75 ± 7% of the WT protein level (Fig. 5*A*), and plasma membrane levels assessed by cell surface biotinylation were directly proportional to total expression (60 ± 10% and 71 ± 6% of WT surface level) (Fig. 5*B*), indicating no significant impacts of the mutations on trafficking or surface presentation.

Saturation analyses (Fig. 5*C*) showed that after normalizing DA transport for relative DAT plasma membrane expression, both mutants possessed significantly lower V_{max} values than the WT protein (WT, 925 ± 34 pmol/min/mg; T53A, 588 ± 53 pmol/min/mg, $p < 0.01$; T53D, 664 ± 53 pmol/min/mg, $p < 0.05$; ANOVA). DA K_m values were not different (WT, 2.0 ± 0.2 μM; T53A, 1.8 ± 0.4 μM; T53D, 1.6 ± 0.1 μM; $p > 0.05$), implicating alteration of transport turnover rate rather than DA recognition as the mechanism for reduced transport in the mutants. To determine if glutamic acid mutation of Thr^{53} would provide a superior phosphomimetic substitution, we generated T53E DAT for analysis in transiently transfected cells. T53E DAT showed comparable expression relative to the WT protein in mAb 16 immunoblots, but in saturation analyses, it showed DA transport V_{max} reductions that were similar in magnitude to that of T53D DAT (not shown), indicating that neither phosphomimetic substitution could rescue the transport reduction seen with the T53A mutation.

To determine if alterations in ion interactions could underlie the reduced V_{max} values obtained with Thr^{53} mutation, we analyzed WT and T53A proteins for Na^+ and Cl^- concentration dependence. In three independent experiments, we found no significant differences in EC_{50} of DA uptake for Na^+ (WT, 84.4 ± 1.5 mM; T53A, 84.3 ± 4.2 mM; $p > 0.05$) or for Cl^- (WT, 58.9 ± 4.6 mM; T53A, 58.5 ± 1.8 mM; $p > 0.05$), indicating that loss of Thr^{53} did not lead to reduced uptake via impacts on the ability of Na^+ or Cl^- to drive DA translocation.

We then used whole-cell superfusion assays to examine the mutants for AMPH-stimulated substrate efflux using [^{3}H]MPP$^+$ as the substrate. MPP$^+$ was robustly transported by the mutants (V_{max} WT, 141 ± 7 pmol/min/mg; T53A, 97 ± 14 pmol/min/mg; T53D, 105 ± 12 pmol/min/mg, $p > 0.05$, $n = 3$), allowing adequate loading of substrate for efflux analysis. Baseline efflux quantified as a fraction of intracellular substrate did not differ between cell lines (Fig. 6). However, although application of AMPH induced robust MPP$^+$ efflux in the WT rDAT-LLCPK$_1$ cells, it produced no detectable substrate release in the rDAT-T53A and T53D cells (Fig. 6). Lack of AMPH-stimulated efflux activity in the mutants is not due to inability to recognize AMPH because 3 μM AMPH inhibited [^{3}H]DA uptake by 75–85% in all three cell lines (not shown). These results suggest that Thr^{53} and/or its ability to undergo phosphorylation/dephosphorylation exert a mechanistic role in inward DA transport and constitute a major prerequisite for AMPH-mediated MPP$^+$ efflux.

DISCUSSION

In this study, we use mass spectrometry and phospho-specific immunostaining as positive function approaches to identify and characterize phosphorylation of DAT Thr^{53} in rodent striatum and heterologous cells. Thr^{53} is present in the membrane-proximal region of the N-terminal tail close to the beginning of transmembrane domain 1 (TM1) in a motif specific for proline-directed kinases, such as ERK1/2, p38 MAPK, and JNK (29). Although we do not yet know which kinase(s) phosphorylate Thr^{53}, our results provide the first evidence that DAT is directly acted on in neurons by this class of enzymes.

The proline-directed kinase with the most well documented effects on DAT is ERK. In cells and striatal tissue, ERK inhibitors induce rapid reductions in DA transport activity (16, 20, 49, 50), whereas activation of D_2 and D_3 DA receptors induces ERK-dependent up-regulation of DAT (7, 51). These findings

indicate that DA transport functionality is positively influenced by tonic ERK signaling and that rapid up-regulation of transport capacity can be achieved by receptor-mediated activation of ERK. Thus, our findings supporting involvement of Thr^{53} in forward and reverse transport suggest a mechanistic basis for regulation of DAT by ERK. Although we previously found no loss of ERK inhibitor effects on uptake activity of T53A DAT (29), the reduced DA transport V_{max} we found in T53A and T53D mutants is consistent with a role for ERK-mediated phosphorylation of Thr^{53} in maintaining transport activity. If future studies support this idea for ERK or related kinases, our estimate that basal phosphorylation of Thr^{53} occurs with a stoichiometry of ~50% suggests a tonic set point readily amenable to either increased or decreased phosphorylation of significant DAT copy numbers to allow robust modulation of transport capacity. Other potential roles for this site could include tyrosine kinase regulation of DAT, which also involves MAPK activity (52), or ERK-associated functions in cocaine and AMPH actions (3, 53). Current efforts are under way in our laboratory to test Thr^{53} phosphorylation in modulating ERK effects on DAT and to investigate potential regulatory inputs from other proline-directed kinases.

Our results also strongly support a role for Thr^{53} phosphorylation in the mechanism of AMPH-stimulated efflux, which is considered to be a crucial factor in the reinforcing and neurotoxic properties of AMPH and related drugs (54). The finding that Thr^{53} exerts a mechanistic role in efflux is striking because the involvement of phosphorylation in reverse transport has previously been attributed to distal N-terminal serines (55). At present, we lack a clear understanding of the relative contributions of these two N-terminal regions in the efflux mechanism and do not know if there is communication between the domains with respect to phosphorylation. However, the importance of the membrane-proximal region of the N terminus in uptake and efflux mechanisms has been shown in several recent mutagenesis studies (6, 56, 57). In particular, the efflux properties of T53A and T53D mutants resemble those found for a SERT construct with the N terminus tethered to the plasma membrane by TAC peptide (56), supporting a crucial role for the precise arrangement and conformational flexibility of the N terminus in the mechanism of transport reversal.

Proline-directed phosphorylation is well established to drive major protein structural rearrangements by inducing cis-isomerization of the peptide backbone around the Ser(P)/Thr(P)–Pro bond (24, 25). This is likely to be the case for DAT as well because ERK phosphorylation of NDAT causes a distinct upward shift in electrophoretic mobility that is not induced by PKC or other AGC kinases (29). Upward shifts in DAT mobility on SDS-polyacrylamide gels induced by phosphorylation conditions have also been noted (16, 45, 58), consistent with altered conformations that could result from Thr^{53}-Pro^{54} cis-isomerization. Phosphorylation of Thr^{53} is thus likely to play a major role in directing the conformational state of the membrane-proximal region of the DAT N terminus.

Our findings that T53A and T53D mutants showed reduced V_{max} for forward DA transport and complete loss of AMPH-stimulated reverse MPP^+ transport strongly support a crucial role for Thr^{53} in the transport mechanism. TM1 of DAT performs an essential role in substrate transport and psychostimulant drug binding (8), and the proximity of Thr^{53} to TM1 suggests the potential for its phosphorylation and/or Thr^{53}-Pro^{54} cis-trans isomerization to impact transport kinetics via effects on TM1 conformation. Alternatively, Thr^{53} phosphorylation and/or Thr^{53}-Pro^{54} cis-trans isomerization could potentially impact the ability of nearby intracellular gate residue Arg^{60} to form a salt bridge with Asp^{436} (59), which could affect molecular transitions necessary for the transport cycle. At present, we cannot distinguish between Thr^{53} contributions to uptake and efflux as due to side chain hydrogen bonding, direct phosphorylation, or peptide backbone cis-trans isomerization. However, if an inability to undergo phosphorylation underlies the transport and efflux reductions seen in T53A DAT, the putative phosphomimetic T53D and T53E mutations do not satisfy the requirements necessary to support these functions. This is probably due to the inability of Asp or Glu to fully compensate for phosphoryl group charge interactions or to induce backbone cis-isomerization.

The proline-rich sequence immediately surrounding Thr^{53} (PPQTP) also constitutes an Src homology 3 (SH3) domain epitope (PXXP) (60) that may serve as a ligand for interactions with SH3 domain proteins. This motif may therefore function to direct DAT oligomer formation or DAT-binding partner interactions (2, 61). Oligomerization is the preferred quaternary state of neurotransmitter transporters (62) and has been shown to play an important role in transporter-mediated efflux (63). DAT oligomerization is also regulated by AMPH (64), suggesting the possibility that AMPH-mediated activation of PKC (65) may regulate DAT monomer-oligomer equilibria through effects on Thr^{53} phosphorylation. In addition, several proteins that affect DA transport and efflux, including syntaxin 1A and receptor for activated protein kinase C1, interact with the DAT N-terminal domain (66–68), suggesting them as possible intermediaries for Thr^{53} effects.

We found strongly increased phosphorylation of DAT Thr^{53} in rat striatal synaptosomes and cells treated with OA, indicating the presence of robust protein phosphatase activity that maintains this residue in the dephosphorylated state (46). The dose of OA used (10 μM) is compatible with inhibition of PP2A and PP1, both of which have been associated with DAT (46, 69). Thr^{53} phosphorylation is also stimulated by PMA; however, PKC cannot directly phosphorylate proline-directed residues (70) and does not phosphorylate NDAT on Thr^{53} *in vitro* (29). Thus, it is likely that stimulation of Thr^{53} phosphorylation by PMA occurs via PKC cross-talk with pathways for ERK or other proline-dependent kinases (71–76). These findings thus demonstrate the ability of Thr^{53} phosphorylation to be regulated either directly via proline-directed kinases and phosphatases or indirectly through PKC modulation of downstream pathways, indicating the potential for Thr^{53} to serve as a locus for integration of DAT regulatory signals. In addition, both OA and PMA induce DAT down-regulation and endocytosis (16), supporting the potential for Thr^{53} phosphorylation to participate in these processes.

Although the structure of the DAT N terminus is unknown, the sequence consists of two Ser/Thr-rich domains in mem-

brane-distal (amino acids 1–21) and membrane-proximal (amino acids 43–64) regions, separated by a charged/hydrophobic sequence devoid of potential phosphate acceptors (amino acids 22–42) (Fig. 2). We have now demonstrated that DAT is phosphorylated by PKC in the membrane-distal region and by proline-directed kinases in the membrane-proximal region (21, 29). Because PKC and other AGC kinases do not act on Ser/Thr residues that precede proline (27, 70, 77), and none of the distal N-terminal serines are present in proline-directed motifs, our findings provide direct evidence that the proximal and distal phosphorylation domains are acted on by functionally distinct classes of protein kinases. This suggests a separation of N-terminal functional mechanisms that may differentially impact transporter regulation and present potential sites for therapeutic modulation of transport activity in dopaminergic diseases.

Acknowledgments—We thank Drs. Amy Newman and John Lever for supplying [^{125}*I]RTI82, Dr. Eric Murphy for supplying SV129 mice, and Drs. Gert Lubec and Wei-Qiang Chen for generous support with mass spectrometry.*

REFERENCES

1. Giros, B., Jaber, M., Jones, S. R., Wightman, R. M., and Caron, M. G. (1996) Hyperlocomotion and indifference to cocaine and amphetamine in mice lacking the dopamine transporter. *Nature* **379,** 606–612
2. Torres, G. E. (2006) The dopamine transporter proteome. *J. Neurochem.* **97,** Suppl. 1, 3–10
3. Lu, L., Koya, E., Zhai, H., Hope, B. T., and Shaham, Y. (2006) Role of ERK in cocaine addiction. *Trends Neurosci.* **29,** 695–703
4. Miller, G. W., Gainetdinov, R. R., Levey, A. I., and Caron, M. G. (1999) Dopamine transporters and neuronal injury. *Trends Pharmacol. Sci.* **20,** 424–429
5. Bannon, M. J., Sacchetti, P., and Granneman, J. G. (1995) in *Psychopharmacology: the fourth generation of progress* (Borroni, E., and Kupfer, D. J., eds) pp. 179–188, Raven Press Ltd., New York
6. Guptaroy, B., Zhang, M., Bowton, E., Binda, F., Shi, L., Weinstein, H., Galli, A., Javitch, J. A., Neubig, R. R., and Gnegy, M. (2009) A juxtamembrane mutation in the N terminus of the dopamine transporter induces preference for an inward facing conformation. *Mol. Pharmacol.* **75,** 514–524
7. Schmitt, K. C., and Reith, M. E. (2010) Regulation of the dopamine transporter. Aspects relevant to psychostimulant drugs of abuse. *Ann. N.Y. Acad. Sci.* **1187,** 316–340
8. Kristensen, A. S., Andersen, J., Jørgensen, T. N., Sørensen, L., Eriksen, J., Loland, C. J., Strømgaard, K., and Gether, U. (2011) SLC6 neurotransmitter transporters. Structure, function, and regulation. *Pharmacol. Rev.* **63,** 585–640
9. Steinkellner, T., Freissmuth, M., Sitte, H. H., and Montgomery, T. (2011) The ugly side of amphetamines. Short- and long-term toxicity of 3,4-methylenedioxymethamphetamine (MDMA, "Ecstasy"), methamphetamine, and D-amphetamine. *Biol. Chem.* **392,** 103–115
10. Sitte, H. H., and Freissmuth, M. (2010) The reverse operation of Na(+)/Cl(−)-coupled neurotransmitter transporters. Why amphetamines take two to tango. *J. Neurochem.* **112,** 340–355
11. Sulzer, D., Sonders, M. S., Poulsen, N. W., and Galli, A. (2005) Mechanisms of neurotransmitter release by amphetamines. A review. *Prog. Neurobiol.* **75,** 406–433
12. Sonders, M. S., Zhu, S. J., Zahniser, N. R., Kavanaugh, M. P., and Amara, S. G. (1997) Multiple ionic conductances of the human dopamine transporter. The actions of dopamine and psychostimulants. *J. Neurosci.* **17,** 960–974
13. Sitte, H. H., Huck, S., Reither, H., Boehm, S., Singer, E. A., and Pifl, C. (1998) Carrier-mediated release, transport rates, and charge transfer induced by amphetamine, tyramine, and dopamine in mammalian cells transfected with the human dopamine transporter. *J. Neurochem.* **71,** 1289–1297
14. Robertson, S. D., Matthies, H. J., and Galli, A. (2009) A closer look at amphetamine-induced reverse transport and trafficking of the dopamine and norepinephrine transporters. *Mol. Neurobiol.* **39,** 73–80
15. Zahniser, N. R., and Doolen, S. (2001) Chronic and acute regulation of Na^+/Cl^--dependent neurotransmitter transporters. Drugs, substrates, presynaptic receptors, and signaling systems. *Pharmacol. Ther.* **92,** 21–55
16. Ramamoorthy, S., Shippenberg, T. S., and Jayanthi, L. D. (2011) Regulation of monoamine transporters. Role of transporter phosphorylation. *Pharmacol. Ther.* **129,** 220–238
17. Vaughan, R. A., Huff, R. A., Uhl, G. R., and Kuhar, M. J. (1997) Protein kinase C-mediated phosphorylation and functional regulation of dopamine transporters in striatal synaptosomes. *J. Biol. Chem.* **272,** 15541–15546
18. Garcia, B. G., Wei, Y., Moron, J. A., Lin, R. Z., Javitch, J. A., and Galli, A. (2005) Akt is essential for insulin modulation of amphetamine-induced human dopamine transporter cell surface redistribution. *Mol. Pharmacol.* **68,** 102–109
19. Fog, J. U., Khoshbouei, H., Holy, M., Owens, W. A., Vaegter, C. B., Sen, N., Nikandrova, Y., Bowton, E., McMahon, D. G., Colbran, R. J., Daws, L. C., Sitte, H. H., Javitch, J. A., Galli, A., and Gether, U. (2006) Calmodulin kinase II interacts with the dopamine transporter C terminus to regulate amphetamine-induced reverse transport. *Neuron* **51,** 417–429
20. Morón, J. A., Zakharova, I., Ferrer, J. V., Merrill, G. A., Hope, B., Lafer, E. M., Lin, Z. C., Wang, J. B., Javitch, J. A., Galli, A., and Shippenberg, T. S. (2003) Mitogen-activated protein kinase regulates dopamine transporter surface expression and dopamine transport capacity. *J. Neurosci.* **23,** 8480–8488
21. Foster, J. D., Pananusorn, B., and Vaughan, R. A. (2002) Dopamine transporters are phosphorylated on N-terminal serines in rat striatum. *J. Biol. Chem.* **277,** 25178–25186
22. Cervinski, M. A., Foster, J. D., and Vaughan, R. A. (2005) Psychoactive substrates stimulate dopamine transporter phosphorylation and down-regulation by cocaine-sensitive and protein kinase C-dependent mechanisms. *J. Biol. Chem.* **280,** 40442–40449
23. Granas, C., Ferrer, J., Loland, C. J., Javitch, J. A., and Gether, U. (2003) N-terminal truncation of the dopamine transporter abolishes phorbol ester- and substance P receptor-stimulated phosphorylation without impairing transporter internalization. *J. Biol. Chem.* **278,** 4990–5000
24. Lu, K. P., Liou, Y. C., and Zhou, X. Z. (2002) Pinning down proline-directed phosphorylation signaling. *Trends Cell Biol.* **12,** 164–172
25. Lu, K. P., and Zhou, X. Z. (2007) The prolyl isomerase PIN1. A pivotal new twist in phosphorylation signaling and disease. *Nat. Rev. Mol. Cell Biol.* **8,** 904–916
26. Ando, S., Ikuhara, T., Kamata, T., Sasaki, Y., Hisanaga, S., Kishimoto, T., Ito, H., and Inagaki, M. (1997) Role of the pyrrolidine ring of proline in determining the substrate specificity of cdc2 kinase or cdk5. *J. Biochem.* **122,** 409–414
27. Gray, C. H., and Barford, D. (2003) Getting in the ring. Proline-directed substrate specificity in the cell cycle proteins Cdc14 and CDK2-cyclinA3. *Cell Cycle* **2,** 500–502
28. Brown, N. R., Noble, M. E., Endicott, J. A., and Johnson, L. N. (1999) The structural basis for specificity of substrate and recruitment peptides for cyclin-dependent kinases. *Nat. Cell Biol.* **1,** 438–443
29. Gorentla, B. K., Moritz, A. E., Foster, J. D., and Vaughan, R. A. (2009) Proline-directed phosphorylation of the dopamine transporter N-terminal domain. *Biochemistry* **48,** 1067–1076
30. Lever, J. R., Carroll, F. I., Patel, A., Abraham, P., Boja, J. W., Lewin, A. H., and Lew, R. (1993) Radiosynthesis of a photoaffinity probe for the cocaine receptor of the dopamine transporter. 3-(*p*-Chlorophenyl)tropan-2-carboxylic acid *m*-([^{125}I]-iodo)-*p*-azidophenethyl ester ([^{125}I]RTI-82). *J. Labelled Compd. Radiopharm.* **33,** 1131–1137
31. Gu, H., Wall, S. C., and Rudnick, G. (1994) Stable expression of biogenic amine transporters reveals differences in inhibitor sensitivity, kinetics, and ion dependence. *J. Biol. Chem.* **269,** 7124–7130
32. Yang, J. W., Vacher, H., Park, K. S., Clark, E., and Trimmer, J. S. (2007)

Trafficking-dependent phosphorylation of Kv1.2 regulates voltage-gated potassium channel cell surface expression. *Proc. Natl. Acad. Sci. U.S.A.* **104,** 20055–20060
33. Zheng, J. F., Patil, S. S., Chen, W. Q., An, W., He, J. Q., Höger, H., and Lubec, G. (2009) Hippocampal protein levels related to spatial memory are different in the Barnes maze and in the multiple T-maze. *J. Proteome Res.* **8,** 4479–4486
34. Gaffaney, J. D., and Vaughan, R. A. (2004) Uptake inhibitors but not substrates induce protease resistance in extracellular loop two of the dopamine transporter. *Mol. Pharmacol.* **65,** 692–701
35. Foster, J. D., and Vaughan, R. A. (2011) Palmitoylation controls dopamine transporter kinetics, degradation, and protein kinase C-dependent regulation. *J. Biol. Chem.* **286,** 5175–5186
36. Vaughan, R. A., Sakrikar, D. S., Parnas, M. L., Adkins, S., Foster, J. D., Duval, R. A., Lever, J. R., Kulkarni, S. S., and Hauck-Newman, A. (2007) Localization of cocaine analog [^{125}I]RTI 82 irreversible binding to transmembrane domain 6 of the dopamine transporter. *J. Biol. Chem.* **282,** 8915–8925
37. Vaughan, R. A., and Kuhar, M. J. (1996) Dopamine transporter ligand binding domains. Structural and functional properties revealed by limited proteolysis. *J. Biol. Chem.* **271,** 21672–21680
38. Foster, J. D., Adkins, S. D., Lever, J. R., and Vaughan, R. A. (2008) Phorbol ester induced trafficking-independent regulation and enhanced phosphorylation of the dopamine transporter associated with membrane rafts and cholesterol. *J. Neurochem.* **105,** 1683–1699
39. Lin, Z., Itokawa, M., and Uhl, G. R. (2000) Dopamine transporter proline mutations influence dopamine uptake, cocaine analog recognition, and expression. *FASEB J.* **14,** 715–728
40. Henry, L. K., Iwamoto, H., Field, J. R., Kaufmann, K., Dawson, E. S., Jacobs, M. T., Adams, C., Felts, B., Zdravkovic, I., Armstrong, V., Combs, S., Solis, E., Rudnick, G., Noskov, S. Y., DeFelice, L. J., Meiler, J., and Blakely, R. D. (2011) A conserved asparagine residue in transmembrane segment 1 (TM1) of serotonin transporter dictates chloride-coupled neurotransmitter transport. *J. Biol. Chem.* **286,** 30823–30836
41. Scholze, P., Nørregaard, L., Singer, E. A., Freissmuth, M., Gether, U., and Sitte, H. H. (2002) The role of zinc ions in reverse transport mediated by monoamine transporters. *J. Biol. Chem.* **277,** 21505–21513
42. Scholze, P., Sitte, H. H., and Singer, E. A. (2001) Substantial loss of substrate by diffusion during uptake in HEK-293 cells expressing neurotransmitter transporters. *Neurosci. Lett.* **309,** 173–176
43. Wu, X., and Gu, H. H. (1999) Molecular cloning of the mouse dopamine transporter and pharmacological comparison with the human homologue. *Gene* **233,** 163–170
44. Giros, B., el Mestikawy, S., Bertrand, L., and Caron, M. G. (1991) Cloning and functional characterization of a cocaine-sensitive dopamine transporter. *FEBS Lett.* **295,** 149–154
45. Vaughan, R. A. (2004) Phosphorylation and regulation of psychostimulant-sensitive neurotransmitter transporters. *J. Pharmacol. Exp. Ther.* **310,** 1–7
46. Foster, J. D., Pananusorn, B., Cervinski, M. A., Holden, H. E., and Vaughan, R. A. (2003) Dopamine transporters are dephosphorylated in striatal homogenates and *in vitro* by protein phosphatase 1. *Brain Res. Mol. Brain Res.* **110,** 100–108
47. Foster, J. D., Cervinski, M. A., Gorentla, B. K., and Vaughan, R. A. (2006) Regulation of the dopamine transporter by phosphorylation. *Handb. Exp. Pharmacol.*, 197–214
48. Li, L. B., Chen, N., Ramamoorthy, S., Chi, L., Cui, X. N., Wang, L. C., and Reith, M. E. (2004) The role of *N*-glycosylation in function and surface trafficking of the human dopamine transporter. *J. Biol. Chem.* **279,** 21012–21020
49. Carvelli, L., Morón, J. A., Kahlig, K. M., Ferrer, J. V., Sen, N., Lechleiter, J. D., Leeb-Lundberg, L. M., Merrill, G., Lafer, E. M., Ballou, L. M., Shippenberg, T. S., Javitch, J. A., Lin, R. Z., and Galli, A. (2002) PI 3-kinase regulation of dopamine uptake. *J. Neurochem.* **81,** 859–869
50. Zapata, A., Kivell, B., Han, Y., Javitch, J. A., Bolan, E. A., Kuraguntla, D., Jaligam, V., Oz, M., Jayanthi, L. D., Samuvel, D. J., Ramamoorthy, S., and Shippenberg, T. S. (2007) Regulation of dopamine transporter function and cell surface expression by D3 dopamine receptors. *J. Biol. Chem.* **282,** 35842–35854
51. Lee, F. J., Pei, L., Moszczynska, A., Vukusic, B., Fletcher, P. J., and Liu, F. (2007) Dopamine transporter cell surface localization facilitated by a direct interaction with the dopamine D2 receptor. *EMBO J.* **26,** 2127–2136
52. Hoover, B. R., Everett, C. V., Sorkin, A., and Zahniser, N. R. (2007) Rapid regulation of dopamine transporters by tyrosine kinases in rat neuronal preparations. *J. Neurochem.* **101,** 1258–1271
53. Shi, X., and McGinty, J. F. (2006) Extracellular signal-regulated mitogen-activated protein kinase inhibitors decrease amphetamine-induced behavior and neuropeptide gene expression in the striatum. *Neuroscience* **138,** 1289–1298
54. Sulzer, D. (2011) How addictive drugs disrupt presynaptic dopamine neurotransmission. *Neuron* **69,** 628–649
55. Khoshbouei, H., Sen, N., Guptaroy, B., Johnson, L., Lund, D., Gnegy, M. E., Galli, A., and Javitch, J. A. (2004) N-terminal phosphorylation of the dopamine transporter is required for amphetamine-induced efflux. *PLoS Biol.* **2,** E78
56. Sucic, S., Dallinger, S., Zdrazil, B., Weissensteiner, R., Jørgensen, T. N., Holy, M., Kudlacek, O., Seidel, S., Cha, J. H., Gether, U., Newman, A. H., Ecker, G. F., Freissmuth, M., and Sitte, H. H. (2010) The N terminus of monoamine transporters is a lever required for the action of amphetamines. *J. Biol. Chem.* **285,** 10924–10938
57. Guptaroy, B., Fraser, R., Desai, A., Zhang, M., and Gnegy, M. E. (2011) Site-directed mutations near transmembrane domain 1 alter conformation and function of norepinephrine and dopamine transporters. *Mol. Pharmacol.* **79,** 520–532
58. Huff, R. A., Vaughan, R. A., Kuhar, M. J., and Uhl, G. R. (1997) Phorbol esters increase dopamine transporter phosphorylation and decrease transport V_{max}. *J. Neurochem.* **68,** 225–232
59. Kniazeff, J., Shi, L., Loland, C. J., Javitch, J. A., Weinstein, H., and Gether, U. (2008) An intracellular interaction network regulates conformational transitions in the dopamine transporter. *J. Biol. Chem.* **283,** 17691–17701
60. Mayer, B. J. (2001) SH3 domains. Complexity in moderation. *J. Cell Sci.* **114,** 1253–1263
61. Egaña, L. A., Cuevas, R. A., Baust, T. B., Parra, L. A., Leak, R. K., Hochendoner, S., Peña, K., Quiroz, M., Hong, W. C., Dorostkar, M. M., Janz, R., Sitte, H. H., and Torres, G. E. (2009) Physical and functional interaction between the dopamine transporter and the synaptic vesicle protein synaptogyrin-3. *J. Neurosci.* **29,** 4592–4604
62. Sitte, H. H., Farhan, H., and Javitch, J. A. (2004) Sodium-dependent neurotransmitter transporters. Oligomerization as a determinant of transporter function and trafficking. *Mol. Interv.* **4,** 38–47
63. Seidel, S., Singer, E. A., Just, H., Farhan, H., Scholze, P., Kudlacek, O., Holy, M., Koppatz, K., Krivanek, P., Freissmuth, M., and Sitte, H. H. (2005) Amphetamines take two to tango. An oligomer-based counter-transport model of neurotransmitter transport explores the amphetamine action. *Mol. Pharmacol.* **67,** 140–151
64. Chen, N., and Reith, M. E. (2008) Substrates dissociate dopamine transporter oligomers. *J. Neurochem.* **105,** 910–920
65. Giambalvo, C. T. (2003) Differential effects of amphetamine transport *versus* dopamine reverse transport on particulate PKC activity in striatal synaptoneurosomes. *Synapse* **49,** 125–133
66. Lee, K. H., Kim, M. Y., Kim, D. H., and Lee, Y. S. (2004) Syntaxin 1A and receptor for activated C kinase interact with the N-terminal region of human dopamine transporter. *Neurochem. Res.* **29,** 1405–1409
67. Carvelli, L., Blakely, R. D., and DeFelice, L. J. (2008) Dopamine transporter/syntaxin 1A interactions regulate transporter channel activity and dopaminergic synaptic transmission. *Proc. Natl. Acad. Sci. U.S.A.* **105,** 14192–14197
68. Binda, F., Dipace, C., Bowton, E., Robertson, S. D., Lute, B. J., Fog, J. U., Zhang, M., Sen, N., Colbran, R. J., Gnegy, M. E., Gether, U., Javitch, J. A., Erreger, K., and Galli, A. (2008) Syntaxin 1A interaction with the dopamine transporter promotes amphetamine-induced dopamine efflux. *Mol. Pharmacol.* **74,** 1101–1108
69. Bauman, A. L., Apparsundaram, S., Ramamoorthy, S., Wadzinski, B. E.,

Vaughan, R. A., and Blakely, R. D. (2000) Cocaine and antidepressant-sensitive biogenic amine transporters exist in regulated complexes with protein phosphatase 2A. *J. Neurosci.* **20,** 7571–7578
70. Sossin, W. S. (2007) Isoform specificity of protein kinase Cs in synaptic plasticity. *Learn Mem.* **14,** 236–246
71. Brändlin, I., Hübner, S., Eiseler, T., Martinez-Moya, M., Horschinek, A., Hausser, A., Link, G., Rupp, S., Storz, P., Pfizenmaier, K., and Johannes, F. J. (2002) Protein kinase C (PKC)η-mediated PKC μ activation modulates ERK and JNK signal pathways. *J. Biol. Chem.* **277,** 6490–6496
72. Mauro, A., Ciccarelli, C., De Cesaris, P., Scoglio, A., Bouché, M., Molinaro, M., Aquino, A., and Zani, B. M. (2002) PKCα-mediated ERK, JNK, and p38 activation regulates the myogenic program in human rhabdomyosarcoma cells. *J. Cell Sci.* **115,** 3587–3599
73. Clark, J. A., Black, A. R., Leontieva, O. V., Frey, M. R., Pysz, M. A., Kunneva, L., Woloszynska-Read, A., Roy, D., and Black, J. D. (2004) Involvement of the ERK signaling cascade in protein kinase C-mediated cell cycle arrest in intestinal epithelial cells. *J. Biol. Chem.* **279,** 9233–9247
74. Wen-Sheng, W. (2006) Protein kinase C alpha trigger Ras and Raf-independent MEK/ERK activation for TPA-induced growth inhibition of human hepatoma cell HepG2. *Cancer Lett.* **239,** 27–35
75. Guerrero, C., Lecuona, E., Pesce, L., Ridge, K. M., and Sznajder, J. I. (2001) Dopamine regulates Na-K-ATPase in alveolar epithelial cells via MAPK-ERK-dependent mechanisms. *Am. J. Physiol. Lung Cell Mol. Physiol.* **281,** L79–L85
76. Pearson, G., Robinson, F., Beers Gibson, T., Xu, B. E., Karandikar, M., Berman, K., and Cobb, M. H. (2001) Mitogen-activated protein (MAP) kinase pathways. Regulation and physiological functions. *Endocr. Rev.* **22,** 153–183
77. Gold, M. G., Barford, D., and Komander, D. (2006) Lining the pockets of kinases and phosphatases. *Curr. Opin. Struct. Biol.* **16,** 693–701